

# Empirical physical formula for potential energy curves of $^{38-66}\text{Ti}$ isotopes by using neural networks

*S. Akkoyun<sup>a</sup>, T. Bayram<sup>b</sup>, S.O. Kara<sup>c</sup>, N. Yildiz<sup>a</sup>*

*<sup>a</sup>Department of Physics, Cumhuriyet University, Sivas, Turkey*

*<sup>b</sup>Department of Physics, Sinop University, Sinop, Turkey*

*<sup>c</sup>Department of Physics, Nigde University, Nigde, Turkey*

## Abstract

Nuclear shape transition has been actively studied in the past decade. In particular, the understanding of this phenomenon from a microscopic point of view is of great importance. Because of this reason, many works have been employed to investigate shape phase transition in nuclei within the relativistic and non-relativistic mean field models by examining potential energy curves (PECs). In this paper, by using layered feed-forward neural networks (LFNNs), we have constructed consistent empirical physical formulas (EPFs) for the PECs of  $^{38-66}\text{Ti}$  calculated in Hartree-Fock-Bogoliubov (HFB) method with SLy4 Skyrme forces. It has been seen that the PECs obtained by neural network method are compatible with those of HFB calculations.

**Keywords:** Neural networks, empirical physical formula, potential energy curves, phase transition, Hartree-Fock-Bogoliubov method

## 1        **1. Introduction**

2        The study of the structural evolution in atomic nuclei with changing numbers of their  
3        neutron and proton constituents dates back to the early days of the nuclear physics. In the  
4        last decade, a number of theoretical developments have given insights into, and ways to  
5        model, this structural evolution, particularly in transitional regions of rapid change [1, 2].  
6        These breakthroughs involve the concepts of quantum phase transitions (QPTs) and the  
7        critical-point symmetries. A new class of symmetries E(5) and X(5) have been suggested  
8        to describe shape phase transitions in atomic nuclei by Iachello [3, 4]. The E(5) critical-  
9        point symmetry has been found to correspond to the second order transition between U(5)  
10        and O(6), while the X(5) critical-point symmetry has been found to correspond to the first  
11        order transition between U(5) and SU(3). These symmetries was experimentally  
12        identified in the spectrum of  $^{134}\text{Ba}$  [5] and  $^{152}\text{Sm}$  [6].

13        From theoretical point of view, QPTs have been studied within the Interacting Boson  
14        Model (IBM) and the solutions of Bohr-Mottelson differential equations. They are useful  
15        representations for describing QPTs in nuclei. Also, phenomenological mean field  
16        models (e.g, Hartree-Fock-Bogoliubov (HFB) method [7, 8] and relativistic mean field  
17        (RMF) model [9, 10, 11]) have been used to investigate the critical-point nuclei with E(5)  
18        or X(5) symmetry in Ref. [12, 13, 14, 15, 16, 17, 18, 19, 20]. In these studies, potential  
19        energy curves (PECs) obtained from quadrupole constrained calculations have been used  
20        for describing the possible critical-point nuclei. Relatively flat PECs are obtained for  
21        critical-point nuclei with E(5) symmetry, while in nuclei with X(5) symmetry, PECs with  
22        a bump are obtained. It should be noted, however, that one should go beyond a simple  
23        mean field level for a quantitative analysis of QPT in nuclei. For this purpose, some  
24        methods have been utilized in Ref. [21, 22, 23, 24]. The application of these methods for  
25        a systematic study of QPT in nuclei is at present still very time-consuming. Therefore, the  
26        evolution of the PECs along the isotopic or isotonic chains is important and can be used  
27        for qualitative understanding of QPTs in nuclei.

28        In Ref. [19], HFB method with SLy4 Skyrme forces have been employed to  
29        investigate ground-state properties of even-even  $^{38-66}\text{Ti}$  isotopes. The calculated binding  
30        energies and deformations with the Skyrme force were obtained in good agreement with  
31        the available experimental data. In particular, shape evolution of Ti isotopes has been  
32        investigated by using calculated PECs to search E(5) symmetry in Ti isotopes, together

1 with the neutron single-particle levels. Particularly  $^{46}\text{Ti}$  has been suggested as to be  
2 possible critical-point nuclei with E(5) symmetry.

3 Recently, neural networks have emerged with successful applications in many fields,  
4 obtaining potential energy surfaces [25], studying nuclear mass systematic [26],  
5 investigating nucleon separation energies [27], classifying unknown energy levels [28],  
6 estimating the density functional theory energy [29], investigating ground state  
7 geometries [30], mapping potential energy surfaces [31], determination of beta decay half  
8 lives [32] and identifying impact parameter in heavy ion collisions [33]. In this work,  
9 borrowing data from our previous work [19], the PECs for  $^{38-66}\text{Ti}$  isotopes as a function  
10 of quadrupole deformation parameter ( $\beta_2$ ) were obtained by using layered feed-forward  
11 neural networks (LFNNs).

12 Due to the physical phenomena correlated with potential energy curves (PECs) of the  
13 isotopes are characteristically highly non-linear, it may be difficult to construct empirical  
14 physical formulas (EPFs) for binding energy functions. By appropriate operations of  
15 mathematical analysis, derivation of highly non-linear physical functions for binding  
16 energies is of utmost interest. These EPFs would be used for specific purposes in  
17 analyzing PECs. We particularly aim to construct explicit mathematical functional form  
18 of LFNN-EPFs for PECs. While the PECs were intrinsically non-linear, even so training  
19 set LFNN-EPFs successfully fitted these binding energies. Furthermore, testing set  
20 LFNN-EPFs consistently predicted the binding energies. That is, the physical laws  
21 embedded in the data were extracted by the LFNN-EPFs.

22 The letter is organized as follows. In Section 2, the HFB method and numerical  
23 details are given briefly. In Section 3, details on artificial neural networks are given. The  
24 results of this study and discussions are presented in Section 4. Finally, conclusions are  
25 given in Section 5.

26

## 27 **2. HFB Formalism and Numerical Details**

28 In HFB method, many properties of the nuclei can be described in terms of a model of  
29 independent particles which move in an average potential. In the HFB formalism, a two-  
30 body Hamiltonian of a system of fermions can be interpreted in terms of a set of  
31 annihilation and creation operators. The ground state wave function is described as the

1 quasi-particle vacuum and the linear Bogoliubov transformation provides connection  
2 between the quasi-particle operators and the original particle operators. The basic  
3 building blocks of the HFB method are the density matrix and the pairing tensor, and  
4 expectation value of the HFB Hamiltonian could be expressed as energy functional  
5 (Details can be found in [8, 34]). In term of Skyrme forces, the HFB energy has the form  
6 of local energy density functional contains the sum of the mean field and pairing energy  
7 densities. These fields can be calculated in the coordinate space [8, 34].

8 In this work, input data for construction of empirical formula of the PECs obtained  
9 from constrained HFB calculations with SLy4 Skyrme force for Ti isotopes was taken  
10 from Ref. [19]. In this reference, HFB equations have been solved by expanding quasi-  
11 particle wave functions on a harmonic oscillator basis expressed in coordinate space. For  
12 pairing, Lipkin-Nogami method was implemented by performing the HFB calculations  
13 with an additional term included in the HF Hamiltonian. Further details on choosing of  
14 oscillator bases and parameters can be found in Ref. [19].

15

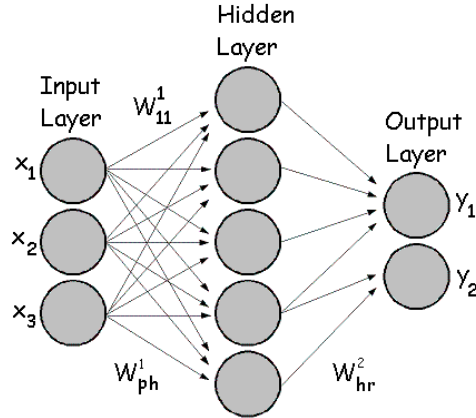
### 16 **3. Artificial Neural Networks**

17 Artificial neural networks (ANNs) are known to be very powerful multivariate tools  
18 that are used when standard techniques fail to properly take account of the correlation  
19 between these variables. The typical goal of the ANN is to get a fast function, which  
20 models well the output of complicated and CPU consuming data. Since trained network is  
21 very fast and does not use neither much memory nor CPU, ANN is well suited for this  
22 task. ANNs offer several advantages, requiring less formal statistical training, ability to  
23 detect complex highly non-linear relationships between input and output variables, ability  
24 to detect all possible interactions between predictor variables. Another benefit of the  
25 ANNs appears in case of existing dataset with a high percentage of missing data.

26

27 ANNs are mathematical models that mimic the human brain. They consist of several  
28 processing units called neurons which have adaptive synaptic weights [35]. ANNs are  
29 also effective tools for pattern recognition. The LFNN which is particular kind of ANN  
30 consists of three layers: input, hidden and output (Fig.1). The number of hidden layers  
31 can differ, but a single hidden layer is enough for efficient non-linear function  
32 approximation [36]. In this study, one input layer with one neuron, one hidden layer with  
33 many ( $h$ ) neuron and one output layer with one neuron ( $1-h-1$ )LFNN topology was used  
for accurately and reliably prediction of the binding energies for even-even  $^{38-66}\text{Ti}$

1 isotopes. Analyses were performed for different hidden neuron numbers,  $h= 4, 9$  and  $14$ .  
 2 The total numbers of adjustable weights were  $8, 18$  and  $28$ .  
 3 where  $p$  and  $r$  are the input and output neuron numbers, respectively.



4

5 **Fig.1.** Three main layers structure of artificial neural networks

6

7 The neuron in the input layer collects the data from environment and transmits via  
 8 weighted connections to the neurons of hidden layer which is needed to approximate any  
 9 non-linear function. The hidden neuron activation function can be theoretically any well-  
 10 behaved non-linear function. In this work, the type of activation function was chosen  
 11 hyperbolic tangent ( $\tanh = (e^x - e^{-x}) / (e^x + e^{-x})$ ) for hidden layer. Finally, the output  
 12 layer neuron returns the signal after the analysis. Note that, an input layer with single  
 13 neuron is firmly equivalent to one neuron LFNN with an appropriate activation function.  
 14 As far as the activation function is analytical, the output is also an analytical function of  
 15 the input.

16 Neural network software NeuroSolutions v6.02 was used [37]. The LFNN inputs  
 17 were quadrupole deformation parameters ( $\beta_2$ ) for  $^{38-66}\text{Ti}$  isotopes and the desired outputs  
 18 were binding energies. As mentioned before, this data for both training and testing stages  
 19 were borrowed from our previous work [19]. For all LFNN processing case, whole data  
 20 were divided into two separate sets, 75% for the training stage and 25% for the testing  
 21 stage. In the training stage, a back-propagation algorithm with Levenberg-Marquardt [38,  
 22 39] for the training of the LFNN was used. By convenient modifications, LFNN modifies  
 23 its weights until an acceptable error level between predicted and desired outputs is

1 attained. The error function which measures the difference between outputs was *mean*  
 2 *square error (MSE)*. Then by using LFNN with final weights, the performance of the  
 3 network is tested over an unseen data. If the predictions of the testing dataset are good  
 4 enough, the LFNN is considered to have consistently learned the functional relationship  
 5 between input and output data [40]. In this study for different  $h$  numbers, the minimum  
 6 MSE values were between 0.0005 and 0.0 for training stage and 0.001 and 0.03 for  
 7 testing stage.

8

### 9 3.1 The tangible algorithm for detector response LFNN-EPF construction

10 In order to construct suitable EPF for highly non-linear PECs, we used one neuron  
 11 output LFNN vector function  $\vec{f}$  as

$$12 \quad \vec{f} : R^p \rightarrow R^r : \vec{f}_k(\vec{x}) = \sum_{j=1}^{h_k} \beta_j G(A_j(\vec{x})), \vec{x} \in R^p, \beta_j \in R, A_j \in A^p, \text{ and } k = 1, \dots, r \quad (1)$$

13 where  $\vec{w}$  is input to hidden layer weight vector,  $\vec{x}$  is the LFNN input vector in Fig. 1,  $b$  is  
 14 the bias weight and  $A^p$  is the set of all functions of  $R^p \rightarrow R$  defined by  $A(\vec{x}) = \vec{w} \cdot \vec{x} + b$ .  
 15 However, this equation is not sufficient for the complete construction of the desired non-  
 16 linear EPF since it gives only the rough structure of the LFNN without generating the  
 17 final EPF parameters/final LFNN optimal weights. Therefore, in order to obtain the final  
 18 weight vector  $\vec{w}_f$  (consisting of the final components of  $w^1$  and  $w^2$  of Fig. 1) and the  
 19 corresponding LFNN output vector function  $\vec{f}_{min} = \vec{f}(\vec{w}_f)$  of Eq. (1), we simultaneously  
 20 used the *MSE values* and Eq. (1). More clearly, given the desired input-output data,  $\vec{f}_{min}$  is  
 21 the network output vector function of Eq. (1) which gives the minimum MSE by a  
 22 convenient LFNN weight adaptation. Note that,  $\vec{f}_{min}$  is the best non-linear estimation  
 23 vector of the theoretically unknown desired output function  $\vec{y} : R^p \rightarrow R^r$ . In other  
 24 saying, the unknown vector function  $\vec{y}$  is estimated by  $\vec{f}_{min}$  which is actually desired non-  
 25 linear EPF that we aim to eventually obtain. Since  $\vec{f}_{min}$  is the highly important quantity,  
 26 we restate it in Eq. (2).

$\vec{f}_{min}$  of this paper : Given input-output data ( $\vec{x}$  and  $\vec{y}$  samples) and final weight vector  $\vec{w}_f$ , LFNN  $\vec{f}_{min} = \vec{f}(\vec{w}_f)$  is our desired binding energy EPF. In this paper, LFNN input was the quadrupole deformation parameters ( $\beta_2$ ). Desired vector  $\vec{y}$  was binding energy. Final details for  $\vec{f}_{min}$  of this paper are given Section 3.3.

(2)

6

### 7 3.3 Final $\vec{f}_{min}$ details

8  $\vec{f}_{min}$  totally depends on the structure of the network output vector function  $\vec{f}$  and the  
 9 final weight vector  $\vec{w}_f$ . In Eq. (1), components of the weight are embedded in  $A(\vec{x})$  and  
 10  $\vec{\beta}$ . In Eq. (1),  $\vec{f}$  depends on the apparent forms of activation and  $A$  functions. In this  
 11 paper, setting  $\vec{\beta} = w^2$  of Fig. 1, activation function is non-linear tangent hyperbolic and  
 12  $A$  is the dot product of  $w^1$  and  $\vec{x}$  of Fig. 1. So, we can construct explicit form of  $\vec{f}$ .  
 13 Afterwards, by minimization of *MSE values*, we finally obtain  $\vec{f}_{min} = \vec{f}(\vec{w}_f)$ . Now, the  
 14 concrete LFNN-EPF construction algorithm for non-linear PECs is completed. The actual  
 15 LFNN-EPFs results are given in Section 4.

16

## 17 4. Results and discussions

18 In figures and text where it suitably applies, the abbreviation *calc* is used for the  
 19 calculated data obtained by HFB theory. As mentioned in Section 3, the LFNN training  
 20 and testing set data used in this paper were borrowed from [19]. Note that, the LFNN  
 21 inputs and outputs used in this paper were explicitly defined in Eq. (1). Inputs were  
 22 quadrupole deformation parameters ( $\beta_2$ ) and the corresponding outputs were binding  
 23 energies of the Ti isotopes. The abbreviation *nno* (neural network output) is for both  
 24 training or testing set results.

25

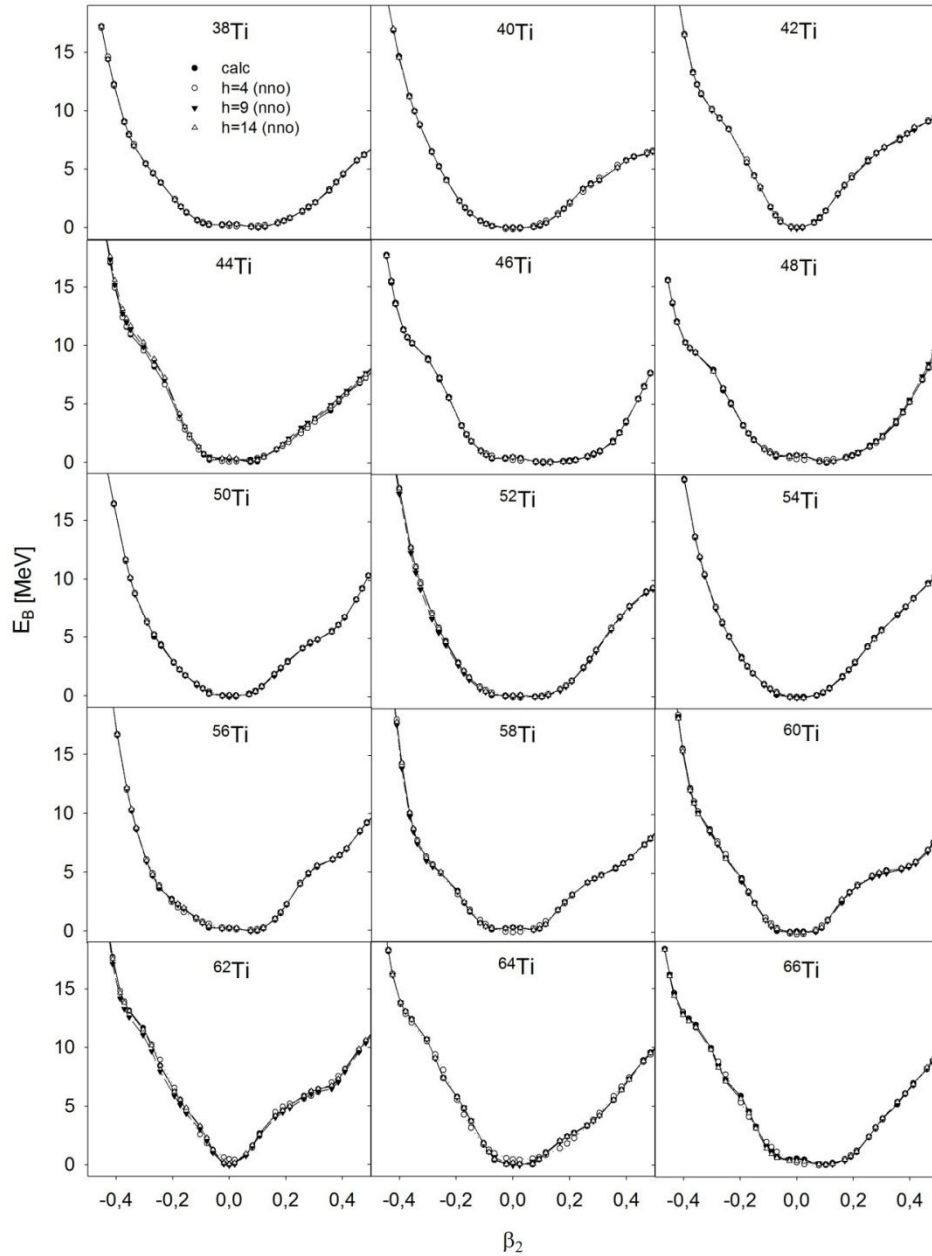
26

## 1           4.1 Training

2           For the PECs, the training set *nno* fittings were given in terms of quadrupole  
3 deformation parameters ( $\beta_2$ ) versus binding energies of the Ti isotopes obtained from  
4 SLy4 Skyrme force (Fig. 2). The LFNN had a single hidden layer with  $h=4, 9, 14$ . The  
5 number of data points belonging to the training stage was about 75% of overall data. It  
6 can be clearly seen in Fig. 2,  $^{42,50,62}\text{Ti}$  isotopes which have shell closure with magic  
7 neutron numbers ( $N=20, N=28$ ) and semi-magic number ( $N=40$ ) were found to be  
8 spherical. Also  $^{40}\text{Ti}$  was found to be spherical while  $^{38}\text{Ti}$  has prolate shape. The PECs of  
9  $^{44}\text{Ti}$  seems relatively flat with a small bump which means that it is possible example of  $\beta$ -  
10 soft nucleus. The PEC of  $^{46}\text{Ti}$  and  $^{48}\text{Ti}$  is flat from  $\beta_2=-0.2$  to  $\beta_2=0.35$  and  $\beta_2=-0.2$  to  
11  $\beta_2=0.2$ , respectively. In both of the PECs, the variations of the total binding energies are  
12 less than 2 MeV through these  $\beta_2$  intervals which implies that the barriers against  
13 deformation are so weak. However, the PECs of  $^{46}\text{Ti}$  is much flatter than those of  $^{48}\text{Ti}$   
14 and the PECs of  $^{48}\text{Ti}$  has a small bump in Fig. 2. This means that  $^{46}\text{Ti}$  should be an  
15 example of critical-point nuclei with E(5) symmetry, while  $^{48}\text{Ti}$  can be thought as an  
16 example of candidate critical-point nuclei with X(5) symmetry. In addition,  $^{54-58}\text{Ti}$  nuclei  
17 have flat PECs with a very small bump, while  $^{52}\text{Ti}$  and  $^{60}\text{Ti}$  have flat PECs. It is possible  
18 argue that  $^{54-58}\text{Ti}$  can be an example of possible critical-point nuclei with X(5) symmetry  
19 while  $^{52}\text{Ti}$  and  $^{60}\text{Ti}$  should be candidate for E(5) symmetry.

20           Moreover in the same figures, one would also concentrate only on comparing specific  
21 *nno* fittings with its corresponding *calc* values. In Fig. 2, the *nno* fittings agree  
22 exceptionally well with highly non-linear *calc* values. Particularly note that, as  
23 principally aimed in this paper, the obtainment of PECs had been successfully made by  
24 the LFNN-EPFs.





1

2

**Fig.2.** HFB calculation (*calc*) with SLy4 Skyrme force and neural network output (*nno*) training set fittings for PECs of different Ti isotopes

3

4

5

6

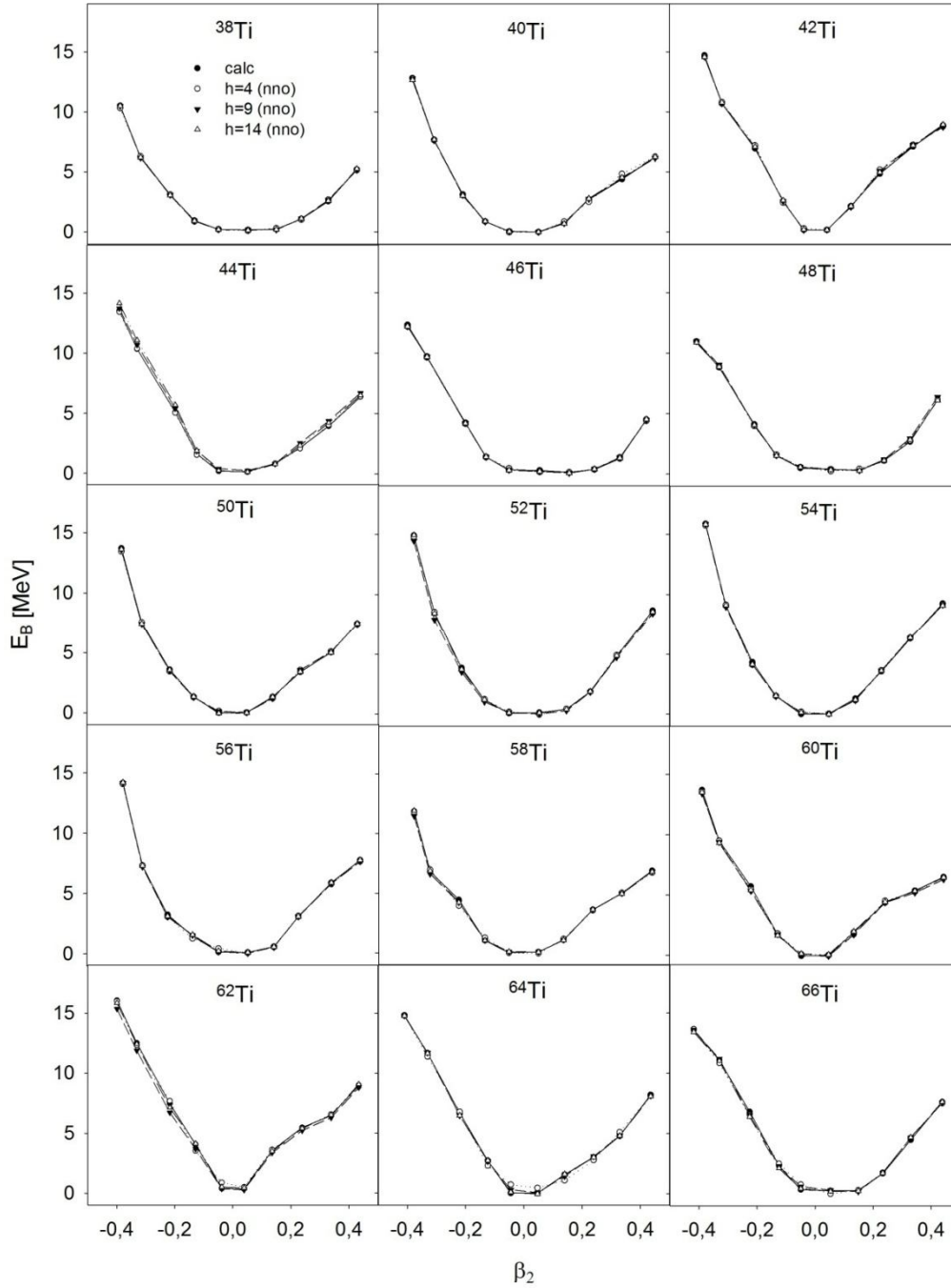
#### 4.2 Testing

7

Unless the training set LFNN-EPFs are further tested over the data, these fitted EPFs cannot be used consistently over a desired range of the data. In other words, if the training sets LFNNs well predict previously unseen testing set data, then the LFNN have regarded to have successfully generalized the data, proving consistent estimations. If the

10

1 estimations are consistent with the testing data values, then the LFNNs can be taken as  
2 appropriate LFNN-EPFs. For the PECs, the corresponding testing set *nno* predictions of  
3 Fig.2 were given in Fig.3. Naturally, the single hidden layer training set LFNNs with  
4  $h=4, 9, 14$  which led to Fig. 2 were also used for *nno* testing set predictions. As can be  
5 seen in Fig.3, the *nno* predictions agree exceptionally well with highly non-linear *calc*  
6 values. This clearly shows that the testing set LFNNs of the quadrupole deformation  
7 parameters ( $\beta_2$ ) versus binding energies of the Ti isotopes have consistently generalized  
8 the training LFNN fittings. Therefore, LFNNs obtained can be safely used as LFNN-  
9 EPFs because the physical law embedded in the quadrupole deformation parameters ( $\beta_2$ )  
10 versus binding energies of the Ti isotopes data has been successfully extracted by the  
11 LFNN constructed. Particularly note that, as principally aimed in this paper, the PECs  
12 have been successfully made by the LFNN-EPFs.



1

2 **Fig.3.** HFB calculation (*calc*) with SLy4 Skyrme force and neural network output (*nno*)  
 3 testing set predictions for PECs of different Ti isotopes

4

## 5 **5. Conclusions and potential applications**

6 In this paper, based on inputs of the PECs obtained from constrained HFB  
 7 calculations with SLy4 Skyrme force for  $^{38-66}\text{Ti}$  isotopes, we generated PECs

1 distributions by using artificial neural networks. The PECs of nuclei can provide  
2 knowledge for qualitatively understanding of QPTs in nuclei. These distributions can  
3 help determination of the nuclear shapes. It is clearly seen that the neural network  
4 method, which can be applied very fast, was consistent with the calculated results. The  
5 advantage of the ANN method is that it does not need any relationship between input and  
6 output data. For highly non-linear binding energies for quadrupole deformation  
7 parameters ( $\beta_2$ ), we have novelly constructed consistent empirical physical formula  
8 (EPFs) by appropriate LFNNs. The testing set LFNNs of the quadrupole deformation  
9 parameters ( $\beta_2$ ) versus binding energies of the Ti isotopes have generalized the training  
10 LFNN fittings. Therefore, the testing set LFNNs can be confidently used as LFNN-EPFs.

11

## 12 **References**

- 13 [1] R. F. Casten, and E. A. McCutchan, "Quantum Phase Transitions and Structural  
14 Evolution in Nuclei", J. Phys. G: Nucl. Part. Phys. 34, 2007, R285-R320.  
15
- 16 [2] P. Cejnar, J. Jolie, and R. F. Casten, "Quantum Phase Transitions in the Shapes of  
17 Atomic Nuclei", Rev. Mod. Phys. 82, 2010, 2155-2212.  
18
- 19 [3] F. Iachello, "Dynamic Symmetries at the Critical Point", Phys. Rev. Lett. 85 (2000)  
20 3580-3583.  
21
- 22 [4] F. Iachello, "Analytic Description of Critical Point Nuclei in a Spherical-Axially  
23 Deformed Shape Phase Transition", Phys. Rev. Lett. 87, (2001) 052502.  
24
- 25 [5] R. F. Casten, and N. V. Zamfir, "Evidence for a Possible E(5) Symmetry in  $^{134}\text{Ba}$ ",  
26 Phys. Rev. Lett. 85, (2000) 3584-3586.  
27
- 28 [6] R. F. Casten and N. V. Zamfir, "Analytic Description of Critical Point Nuclei in a  
29 Spherical-Axially Deformed Shape Phase Transition", Phys. Rev. Lett. 87 (2001)  
30 052503.  
31
- 32 [7] H. Flocard, P. Quentin, A. K. Kerman, and D. Vautherin, "Nuclear Deformation  
33 Energy Curves with the Constrained Hartree-Fock Method", Nucl. Phys. A 203 (1973)  
34 433-472.  
35
- 36 [8] P. Ring and P. Schuck, "The Nuclear Many-Body Problem", Springer-Verlag, Berlin  
37 (1980).  
38
- 39 [9] B. D. Serot and J.D. Walecka, "The Relativistic Nuclear Many-Body Problem", Adv.  
40 Nucl. Phys. 16 (1986) 1-321.

- 1 [10] P. Ring, "Relativistic Mean Field Theory in Finite Nuclei", Prog. Part. Nucl. Phys.  
2 37 (1996) 193-263.  
3
- 4 [11] J. Meng, H. Toki, S. G. Zhou, S. Q. Zhang, W. H. Long, and L. S. Geng,  
5 "Relativistic Continuum Hartree Bogoliubov Theory for Ground-State Properties of  
6 Exotic Nuclei", Prog. Part. Nucl. Phys. 57 (2006) 470-563.  
7
- 8 [12] J. Meng, W. Zhang, S. G. Zhou, H. Toki, and L. S. Geng, "Shape Evolution for Sm  
9 Isotopes in Relativistic Mean-Field Theory, Eur. Phys. J. A25 (2005) 23-27.  
10
- 11 [13] R. Fossion, D. Bonatsos, and G. A. Lalazissis, "E(5), X(5), and Prolate to Oblate  
12 Shape Phase Transitions in Relativistic Hartree-Bogoliubov Theory", Phys. Rev. C 73  
13 (2006) 044310.  
14
- 15 [14] M. Yu, P.-F.Zhang, T.-N.Ruan, and J.-Y. Guo, "Shape Evolution for Ce Isotopes in  
16 Relativistic Mean-Field Theory, Int. J. Mod.Phys. E 15 (2006) 939.  
17
- 18 [15] R. Rodríguez-Guzmán and P. Sarriguren, "E(5) and X(5) Shape Phase Transitions  
19 within a Skyrme-Hartree-Fock + BCS Approach", Phys. Rev. C 76 (2007) 064303.  
20
- 21 [16] J.-Y. Guo, X.Z. Fang, and Z.Q. Sheng, "Shape Phase Transitions and Possible E(5)  
22 Symmetry Nuclei For Ti Isotopes", Int. J. Mod. Phys. E 17, (2008) 539-548.  
23
- 24 [17] A. H. Yilmaz and T. Bayram, "A Detailed Investigation on the Ground-state Nuclear  
25 Properties of Even-even Mo Isotopes by Using the Relativistic Mean Field Approach", J.  
26 Korean. Phys. Soc. 59 (2011) 3329-3336.  
27
- 28 [18] B.-M. Yao and J.-Y.Guo, "Systematic Analysis of Shape Evolution for Mo Isotopes  
29 with Relativistic Mean Field Theory", Mod. Phys. Lett. A 25 (2010) 1177-1186.  
30
- 31 [19] T. Bayram, "An Investigation on Shape Evolution of Ti Isotopes with Hartree-Fock-  
32 Bogoliubov Theory", Mod. Phys. Lett. A 27 (2012) 1250162.  
33
- 34 [20] T. Bayram, "An Investigation on Shape of Te Isotopes Within the Mean Field  
35 Formalism" (in review).  
36
- 37 [21] T. Nikšić, D. Vretenar, G. A. Lalazissis, and P. Ring, "Microscopic Description of  
38 Nuclear Quantum Phase Transitions", Phys. Rev. Lett. 99 (2007) 092502.  
39
- 40 [22] M. Bender and P.-H. Heenen, "Configuration Mixing of Angular-Momentum and  
41 Particle-Number Projected Triaxial Hartree-Fock-Bogoliubov States Using the Skyrme  
42 Energy Density Functional", Phys. Rev. C 78 (2008) 024309.  
43
- 44 [23] J.M. Yao, J. Meng, P. Ring, and D. Vretenar, "Configuration Mixing of Angular-  
45 Momentum-Projected Triaxial Relativistic Mean-Field Wave Functions", Phys. Rev. C  
46 81 (2010) 044311.  
47
- 48 [24] T.R. Rodríguez and J.L. Egido, "Triaxial Angular Momentum Projection and  
49 Configuration Mixing Calculations with the Gogny Force", Phys. Rev. C 81 (2010)  
50 064323.

1

2 [25] A. Bholoa, S.D. Kenny and R. Smith, “A New Approach to Potential Fitting Using  
3 Neural Networks”, Nucl. Instrum.Meth. B, 255 (2007) 1-7.

4 [26] S. Athanassopoulos, E. Mavrommatis, K.A. Gernoth and J.W. Clark, “Nuclear Mass  
5 Systematics Using Neural Networks”, Nucl. Phys. A, 743 (2004) 222-235.

6 [27] S. Athanassopoulos, E. Mavrommatis, K.A. Gernoth and J.W. Clark, “One and Two  
7 Proton Separation Energies from Nuclear Mass Systematics Using Neural Networks”,  
8 arXiv, nucl-th/0509075.

9

10 [28] K. L. Peterson, “Classification of Cm II and Pu I Energy Levels Using Counter  
11 Propagation Neural Networks”, Phys. Rev. A, 44 (1991) 126-138.

12

13 [29] R.M. Balabin and E.I. Lomakina, “Neural Network Approach to Quantum-  
14 Chemistry Data: Accurate Prediction of Density Functional Theory Energies”, The  
15 Journal of Chemical Physics 131, 074104 (2009).

16

17 [30] L.R. Marim, M.R. Lemes and A. Dal Pino Jr., “Ground-State of Silicon Clusters by  
18 Neural Network Assisted Genetic Algorithm”, Tho. Chem, 663 (2003) 159-165.

19

20 [31] Diogo A.R.S. Latino et al., Mapping Potential Energy Surfaces by Neural Networks:  
21 Theethanol/Au(111) interface”, Journal of Electroanalytical Chemistry, 624 (2008) 109-  
22 120.

23

24 [32] N. Costris, E. Mavrommatis, K.A. Gernoth and J.W. Clark, “A Global Model of  
25 Beta(-) Decay Half-Lives Using Neural Networks”, arXiv:nucl-th/0701096v1.

26

27 [33] C. David and J. Aichelin, “Neural Networks Applied to Nuclear Physics”, 4th  
28 International Workshop on Software Engineering, Artificial Intelligence and Expert  
29 Systems for High-energy and Nuclear Physics : AIHENP '95, Pisa, Italy, 3 - 8 Apr 1995,  
30 pp.709-718.

31

32 [34] M. V. Stoitsov, J. Dobaczewski, W. Nazarewicz, and P. Ring, “Axially Deformed  
33 Solution of the Skyrme-Hartree-Fock-Bogolyubov Equations Using the Transformed  
34 Harmonic Oscillator Basis. The Program HFBTHO (v1.66p).”, Comp. Phys. Commun.  
35 167 (2005) 43-63.

36

37 [35] S. Haykin, “Neural Networks: A Comprehensive Foundation”, Prentice-Hall Inc.,  
38 Englewood Cliffs, NJ, USA, 1999.

39 [36] K. Hornik, M. Stinchcombe, H. White, “Multilayer Feedforward Networks are  
40 Universal Approximators”, Neural Networks, 2 (1989) 359-366.

41 [37] Neurosolutions, <http://www.neurosolutions.com/>.

42 [38] K. Levenberg, “A Method for the Solution of Certain Problems in Least Squares,  
43 Quart. Appl. Math., 1944, Vol. 2, pp. 164–168.

44

- 1 [39] D. Marquardt, “An Algorithm for Least-Squares Estimation of Non-linear  
2 Parameters,” SIAM J. Appl. Math., 1963, Vol. 11, pp. 431–441.  
3
- 4 [40] N. Yıldız, “Layered Feedforward Neural Network is Relevant to Empirical Physical  
5 Formula Construction: A Theoretical Analysis and Some Simulation Results”, Phys. Lett.  
6 A 345 (1-3) (2005) 69.